

The hemispherical deflector analyser revisited

II. Electron-optical properties

E.P. Benis^{a,*}, T.J.M. Zouros^{a,b}

^a Institute of Electronic Structure and Laser, P.O. Box 1385, 71110 Heraklion, Crete, Greece

^b Department of Physics, University of Crete, P.O. Box 2208, 71003 Heraklion, Crete, Greece

Received 29 November 2007; received in revised form 31 January 2008; accepted 2 February 2008

Available online 13 February 2008

Abstract

Using the basic spectrometer trajectory equation for motion in an ideal $1/r$ potential derived in Eq. (101) of part I [T.J.M. Zouros, E.P. Benis, J. Electron Spectrosc. Relat. Phenom. 125 (2002) 221], the operational characteristics of a hemispherical deflector analyser (HDA) such as dispersion, energy resolution, energy calibration, input lens magnification and energy acceptance window are investigated from first principles. These characteristics are studied as a function of the entry point R_0 and the nominal value of the potential $V(R_0)$ at entry. Electron-optics simulations and actual laboratory measurements are compared to our theoretical results for an ideal biased paracentric HDA using a four-element zoom lens and a two-dimensional position sensitive detector (2D-PSD). These results should be of particular interest to users of modern HDAs utilizing a PSD.

© 2008 Elsevier B.V. All rights reserved.

PACS: 07.81.+a

Keywords: Electron spectroscopy; ESCA; Hemispherical analyser; Paracentric hemispherical analyser; Fringing fields

1. Introduction

This article is the second part of an in depth investigation focusing on the study of the orbits of non-relativistic charged particles inside a hemispherical deflector analyser (HDA), as well as on the electron-optical properties and optimal operation characteristics of the HDA. The general case of a biased paracentric HDA, i.e., an HDA whose entry is biased at a nominal voltage $V(R_0) \neq 0$ and is paracentric lying at a radial position $R_0 \neq \bar{R} = (R_1 + R_2)/2$, where R_1 and R_2 are the inner and outer radii of the HDA, respectively, is considered. The conventional HDA treated in the literature to date has typically $V(R_0) = 0$ and $R_0 = \bar{R}$. Interest in such a biased paracentric HDA has been prompted by recent articles [1–9] in which electron-optical simulations demonstrated improved focusing and therefore energy resolution for such an HDA. The nature of the effect is attributed to the strong fringing fields at entry. Towards the investigation of this effect, we initially proceed with studying the trajectories

of a charged particle in an *ideal* biased paracentric HDA, i.e., an HDA free of fringing fields.

Thus, in the first review article [10,11] (from here on referred to as paper I), we gave a general treatment of charged particle motion in the *ideal* potential $\tilde{V}(r) = -k/r + c$. The general trajectory equations were obtained in analytic form for r as a function of the deflection angle ω and the launching angle α . In our treatment, the reference (or principal) ray describes an elliptical trajectory starting at $r(\omega = 0) = R_0$ biased at $\tilde{V}_0 \equiv V(r(\omega = 0) = R_0)$ and exiting after deflection through $\Delta\omega = \pi$ at $r(\omega = \pi) = R_\pi$ (see Fig. 3 and Eqs. (90) and (93) in paper I). Conventional HDA trajectory equations [12–18] can be readily recovered as the special case where $R_0 = R_\pi = \bar{R}$ and $\tilde{V}_0 = V_p$, where V_p is the pre-retardation plate voltage of the analyser. The finite potential at the HDA entry \tilde{V}_0 was also found to introduce non-negligible refraction. Thus, a formal treatment of refraction at the idealized sharp potential boundary, represented by a step function potential $V(r, \theta)$, was also included and the basic equation of the analyser was obtained as a function of either α or α^* , the entry angle after or prior to refraction, respectively. The form written in terms of α^* (see Eq. (I101)) was found to be surprisingly simple, much simpler than the one obtained in terms

* Corresponding author. Tel.: +30 2810391127.

E-mail address: benis@iesl.forth.gr (E.P. Benis).

of α (Eqs. (I99) and (I100) in Ref. [10,11]), arguing in favor of using the form with α^* .

In this paper we use the basic analyser trajectory equation for motion in an ideal potential obtained in Eq. (I101) to investigate the electron-optical properties of the generalized HDA such as dispersion, energy resolution, energy calibration and energy acceptance window. We again parameterize our results in terms of the entry radius $r = R_0$ and the nominal bias at entry \tilde{V}_0 . Our results are also compared to electron-optics simulations using the popular ion optics package SIMION [19–21] and to actual laboratory measurements using our own biased paracentric HDA [22–24]. Both SIMION results and real measurements include the effects of the strong fringing fields, whose effects on the electron-optical properties of the HDA are further discussed.

The reader is referred to paper I for the detailed definitions and descriptions of the various variables and parameters introduced. Here we maintain the same notation. For convenience, a definition list of the symbols used here along with their values for our own HDA are given in Table A.1 of the Appendix A.

2. Focusing and dispersive properties of an ideal 1/r potential

The focusing properties of an ideal HDA have already been discussed in many excellent treatments [12–18]. Here we give a brief but generalized [14] approach. A basic optical layout of the spectrograph is shown in Fig. 1. A beam of charged particles emanates from a source of dimension d_s at a pencil angle $\Delta\alpha_s$ defined by the lens pupil entry d_p and its distance l from the source. The source (object) is focused by the lens onto the HDA entry plane having a dimension Δr_0 (image) smaller than the physical opening d_0 of the HDA entry aperture (for 100% transmission). Pre-retardation changes the energy of the central ray from T at the source to t just prior to HDA entry. The image Δr_0 , which is associated with the maximum HDA entry half-angle α_m^* and α_m (after refraction), is finally imaged after dispersion at the exit plane of the HDA and is detected by a 2D-PSD.

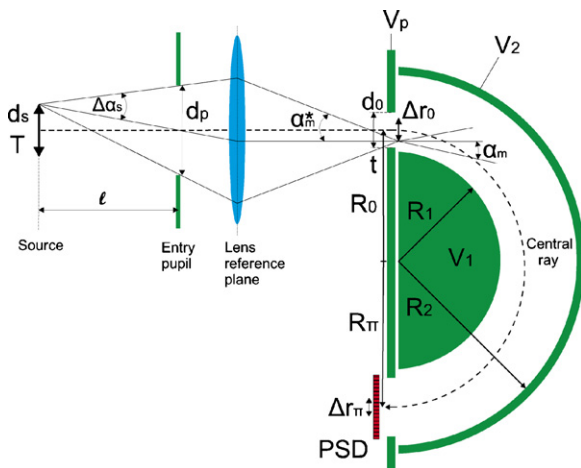


Fig. 1. Schematic geometry of typical HDA spectrograph equipped with a focusing/deceleration lens system and a 2D-PSD. The drawing has been simplified by approximating the (thick) lens by a thin lens. The vertical dimensions are particularly enhanced.

Since the HDA focusing properties can be studied from the ray trace on the exit plane [8,9,25], an expression which gives the position of the particle at the exit, as a function of its position and direction at the entry and its reduced pass energy τ is needed. This equation was derived in detail in paper I [10,11] (see Eq. (I102)) to be:

$$r_\pi = -r_0 + \frac{R_0(1 + \xi)}{1 + (\xi/\gamma)(1 - \tau \cos^2 \alpha^*)}, \quad (\text{ideal HDA}) \quad (1)$$

where (from I) r_0 and r_π are the entry and exit radii, respectively, of the particle trajectory. $\xi \equiv R_\pi/R_0$ is the paracentricity of the HDA, with R_0 and R_π the entry and exit radius of the principal trajectory, respectively. In practice, we shall always take R_π to be the mean radius of the HDA, i.e., $R_\pi = \bar{R} = (R_1 + R_2)/2$, however the symbol R_π is maintained throughout for generality. A charged particle having an initial energy T is decelerated prior to dispersion through the HDA to a pass energy of t , so that $t \equiv T - qV_p$. w is the nominal “tuning” energy, i.e., the energy of the principal trajectory, after preretardation. Thus, the reduced pass energy is defined as $\tau \equiv t/w$. Finally, γ is defined such that $q\tilde{V}(R_0) = (1 - \gamma)w$. Note that, for a conventional HDA, $\tilde{V}(R_0) = 0$ and $R_0 = R_\pi$, so that $\xi = 1$ and $\gamma = 1$. Eq. (1) is known [26] as the *basic equation* of the spectrograph.

For an *ideal* biased HDA one also needs to consider particle refraction at the HDA entry, as discussed in detail in I. In our step potential model presented in I, refraction was found to result in a change of both kinetic energy (Eq. (I B.21)) and angle (Eq. (I B.22)) as the particle crosses the entry plane from a potential $V = 0$ to one of $V = V(r_0)$. Thus, a particle with kinetic energy $K^* = t$ and angle α^* prior to refraction at entry, will have after refraction, an energy $K = t - q\tilde{V}(r_0)$ and angle given by $\sin \alpha = \sqrt{t/K} \sin \alpha^*$. For $t = w$ and $r_0 = R_0$, we note that $K = w - q\tilde{V}_0 = \gamma w$ and therefore $\alpha^* \approx \gamma \alpha$ in the small angle approximation. Thus, for $\gamma > 1$, $K > K^*$ and $\alpha < \alpha^*$, the particle will in general be accelerated to larger kinetic energies and refracted to smaller angles within the HDA. These changes will influence somewhat the overall performance of the HDA.

Next, we study the basic focusing and dispersion properties of an *ideal* hemispherical spectrograph based on Eq. (1). The effects of the strong fringing field [1,6–9] are only discussed in as much as the results obtained for the ideal HDA disagree with comparisons to SIMION simulations and laboratory measurements.

2.1. Magnification, dispersion and angular aberrations

In general, the Taylor expansion of the change in exit radial position Δr_{exit} up to first order in energy change and up to second order in the angular terms takes the unique form for an electrostatic analyser given by [12–14,26]:

$$\Delta r_{\text{exit}} \equiv \mathcal{M}\Delta r_{\text{entry}} + D\frac{\Delta\tau}{\tau} + P_1\alpha^* + P_2\alpha^{*2} + \dots \quad (2)$$

In particular, using the symbols introduced here for the HDA and after a deflection of 180° we may identify r_{exit} with r_π and

Download English Version:

<https://daneshyari.com/en/article/5396892>

Download Persian Version:

<https://daneshyari.com/article/5396892>

[Daneshyari.com](https://daneshyari.com)